PROCEEDINGS OF THE INTERNATIONAL CONFERENCE
NANOMATERIALS: APPLICATIONS AND PROPERTIES
Vol. **2** No 1, 01NTF02(3pp) (2013)

Characterization of Ti-B-C-N Nanocomposite Coatings

V.I. Ivashchenko[1,*], P.L. Scrynskyy[1], A.I. Kuzmichev[2], L.A. Ivashchenko[1], O.Yu. Khyzhun[1], I.I. Timofejeva[1], O.O. Butenko[1], V.M. Granko[1]

[1] *Institute of Problems of Material Science, NAS of Ukraine, Krzhyzhanovsky str. 3, 03142 Kyiv, Ukraine*
[2] *National Technical University "Kyiv Polytechnic Institute", bul. Peremoga, 37, 03056 Kyiv, Ukraine*

(Received 02 August 2013; published online 29 August 2013)

Nanocomposite Ti-B-N-C coatings were deposited by magnetron sputtering of TiN and B_4C targets in the argon-nitrogen atmosphere at different nitrogen flow rates (F_{N2}). The structure, chemical bonding and mechanical properties were investigated. The results of the investigations of the nanocomposite, TiN and BCN coatings show that the Ti-B-C-N coatings consist of the TiNC nanocrystals (3.4 – 6.5 nm) embedded into the amorphous matrix that consists of amorphous boron nitrogen (a-BN) and amorphous carbon (a-C). The coatings contain a small admixture of titanium oxides that are aggregated at the grain boundaries. The coatings deposited at high nitrogen flow rates were textured. An introduction of nitrogen prompts the formation of the nanocrystallites of the TiN-TiC solid solutions and the a-BN amorphous tissue, which, in turn, causes the improvement of the mechanical properties of the Ti-B-C-N coatings. The best samples exhibited nanohardnes above 39 GPa.

Keywords: Magnetron Sputtering, TiN/BCN Nanolayered Coatings, Nanohardness, Knoop Hardness, Microstructure, Chemical Bonding.

PACS numbers: 81.15.– z, 81.15.Cd

1. INTRODUCTION

Nanocomposite coatings are widely used for surface hardening of cutting tools due to high hardness, good corrosion stability and low friction coefficient [1]. The TiN-BN based nanocomposite coatings were studied in Refs. [2, 3]. The nc-TiN/a-BN, nc-TiN/a-BN/a-TiB_2 and nc-TiN/a-TiB_x/a-BN coatings were prepared using the plasma enhanced chemical vapor deposition (PECVD) method and arc vacuum evaporation. It was established that hardness of such coatings reached above 40 – 50 GPa, when the size of TiN nanocrystallites was in the range of 3 – 6 nm, and the amorphous grain boundaries represented one amorphous monolayer (ML) of BN [3]. An insignificant change of the thickness of this layer led to drastic reducing hardness. The Ti-B-C-N coatings were deposited by magnetron sputtering the TiB_2 and TiC targets [4]; Ti, C and B_4C targets [5]; composite Ti + B_4C target [6]; as well by a PECVD technique using a gaseous mixture of $TiCl_4$, BCl_3, CH_4, Ar, N_2 and H_2 [7]. We did not find any investigations of the Ti-B-C-N coatings prepared by using the TiN and TiB_4 targets. Therefore we have deposited the series of Ti-B-C-N coatings using such targets to improve coating properties and to investigate an influence of nitrogen flow rate on the structural and mechanical properties of the deposited coatings.

2. EXPERIMENTAL DETALIES

The Ti-B-C-N coatings were prepared by reactive DC magnetron sputtering the TiN and B_4C targets at the following deposition parameters: substrate temperature T_S = 350 °C; substrate bias U_D = 50 V; flow rate (F) F_{N2} = 0 (SPM-09), 2 (SPM-10), 4 (SPM-11), 7.5 (SPM-12) sccm; F_{N2} + F_{Ar} = 42 sccm; working pressure P_C = 1.0 mTorr; current I (B_4C target) = 100 mA; I (Ti target) = 200 mA; sputtering time t = 60 min. A base pressure was ~ 10^{-6} Torr. The targets were synthesized using a self-propagating high-temperature synthesis consolidation method. The coatings were deposited on silicon (001) single crystal wafers. The same parameters were used to prepare the BCN and TiN coatings, for except, F_{N2} = 0 (TiN) and F_{Ar} = 60 and F_{N2} = 20 sccm (BCN).

To identify coating structures, X-ray diffraction (XRD, DRON-3) and X-ray photoelectron spectroscopy (XPS, UHV-Analysis-System assembled by SPECS) investigations were carried out. The nanohardness (H) and elastic modulus (E) were determined through indentation tests by the Nanoindenter-G200 instrument equipped with a Berkovich pyramidal tip. Fourier transform infrared (FTIR) spectra were measured with a spectrometer SPECORD M80. The thickness of the coatings was determined with an optic profilometer. The thickness was 1.0, 0.6, 0.5 and 0.4 μm for SPM-09, SPM-10, SPM-11 and SPM-12, respectively, and 0.4 and 0.5 μm for SP-08 and SP-13, respectively.

3. RESULTS AND DISCUSSION

The FTIR spectra of the BCN coatings are shown in Fig. 1. The absorption bands at 780 cm^{-1} and 1376 cm^{-1} are caused by the B-N bonds in hexagonal (h) boron nitride h-BN [8]. The band at 1106 cm^{-1} can be assigned to the B-N bonds in cubic boron nitride c-BN and to the B-C bonds in B_4C [8,9]. The B-C and C=N bonds are reported to be found at approximately 1500 cm^{-1} [8]. The broad absorption band around 3400 cm^{-1} is due to the vibration of the O-H bonds [8]. It follows that the

*ivash@ipms.kiev.ua

coatings deposited by sputtering the B_4C target have mainly the B-N network and contain small B-C and O-H fragments. The nanohardness and elastic modulus of the BCN coatings are ~ 10 GPa and ~ 100 GPa, respectively.

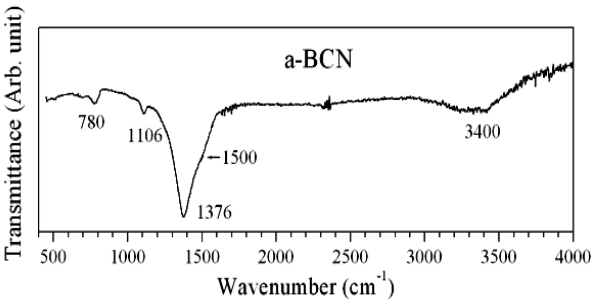

Fig. 1 – FTIR spectra of the BCN coating

The XRD spectra of the deposited Ti-B-C-N coatings are shown in Fig. 2. The position of the XRD peaks points to the formation of the TiC-TiN solid solutions (TiNC). In the sequence SPM-09 – SP-12, the intensity of the XRD TiNC (111) reflection decreases, and the intensity of the TiNC (200) reflection increases. Only one TiNC (002) peak is observed in the XRD spectra of both SPM-12 and SPM-13 samples. The grain size evaluated from the Scherrer formala was 6.5, 6.0, 4.3 and 3.4 nm for SPM-09, -10, -11 and -12, respectively, and 8.5 nm for SPM-13. One can see that increase in nitrogen flow rate leads to reducing the mean grain size.

Typical X-ray photoelectron spectra of core levels for the Ti-B-C-N coatings are presented in Fig. 3. The B 1s peak at 191.2 eV and the broad maximum at 200 eV correspond to the B-N bonds in h-BN [10]. The availability of the maximum at 200 eV indicates that the B-N bonds in c-BN are missing [10]. In the N 1s spectrum, the main peak at 396.9 eV is caused by the energy losses in TiN [11]. The peak asymmetry towards the higher bonding energies can be assigned to the N-B (398.5 eV) and N-C (399.3 eV) bonds [8]. The C 1s spectrum is mainly formed with the C-C bonds (285 eV) as well with the C-N and C-O bonds (286 – 285 eV) [8, 12]. The absence of any feature around 283 eV points out that, in the coatings, the B-C interaction is not realized [8]. The shoulder at ~ 455.6 eV originate from the Ti $2p^{3/2}$ levels in TiN, whereas, two peaks around ~ 458.6 eV and ~ 464.0 eV are due to the Ti $2p^{3/2}$ and Ti $2p^{1/2}$ levels in TiO_2, respectively [12].

Thus, the results of the XRD and XPS investigations of the deposited nanocomposite coatings and TiN and BCN monolayer coatings show that the Ti-B-C-N coatings most likely have the following structure: nc-TiNC/a-BN+a-C, i.e., they consist of the TiNC nanocrystallites embedded into the amorphous BN (a-BN) matrix that contain amorphous carbon (a-C). The coatings contain a small admixture of titanium oxides that are aggregated at the grain boundaries.

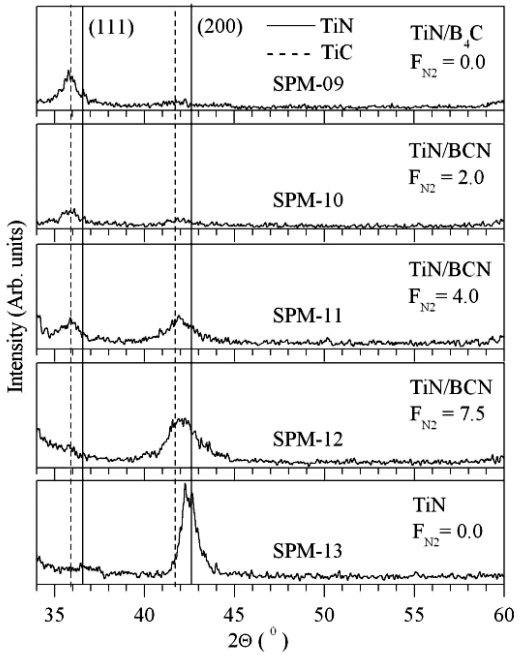

Fig. 2 – XRD spectra of the Ti-B-C-N coatings. The vertical lines denote the TiN and TiC reflection lines according to PDF files [065-0970], [032-1381]

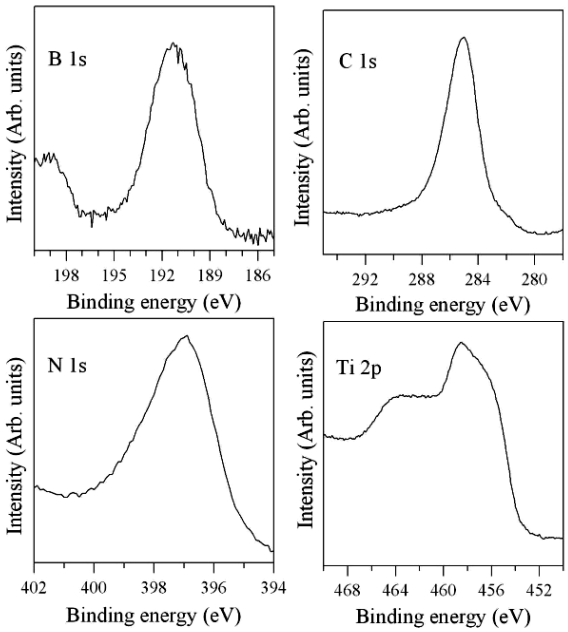

Fig. 3 – Typical XPS spectra of core levels for Ti-B-C-N coatings after etching in argon for 5 min

In Fig. 4, the dependencies of the nanohardness and elastic modulus of the deposited coatings on nanoindenter penetration are presented. In Fig. 5 we show these values as functions of nitrogen flow rates. One can see that the hardness and elastic modulus of the Ti-B-C-N coating, deposited at the highest flow rate of 7.5 sccm, are largest. This means that the formation of the TiN-TiC solid solutions and the a-BN amorphous tissue caused by nitrogen incorporation results in the improvement of the mechanical properties of the Ti-B-C-N coatings. It should be noted that the values of H

and E of all the Ti-B-C-N coatings are much higher than those of TiN coatings (Fig. 4).

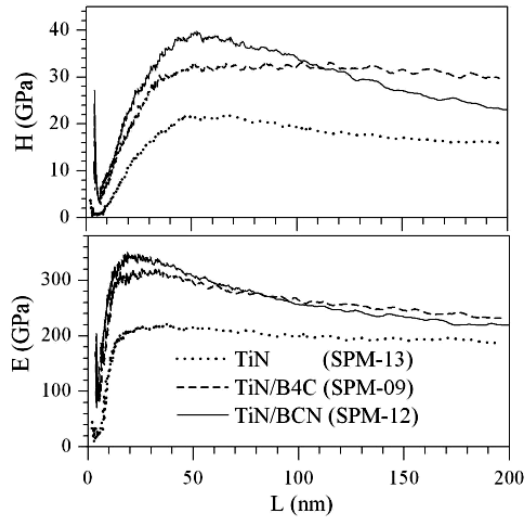

Fig. 4. – Nanohardness (H) and elastic modulus (E) of the TiN and Ti-B-C-N coatings as functions of nanoindenter penetration

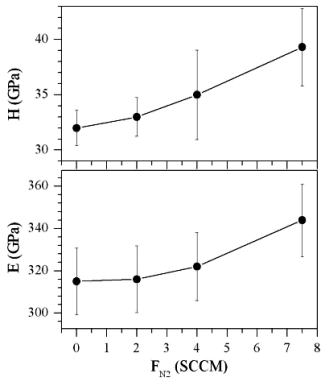

Fig. 5. – Nanohardness (H) and elastic modulus (E) as functions of nitrogen flow rate (F_{N2}) for the Ti-B-C-N coatings

The nanocomposite Ti-B-C-N coatings deposited at comparatively low substrate temperatures (below 350 °C) could be recommended for an introduction to industry as wear-resistant and protective coatings.

4. CONCLUSIONS

We deposited and investigated Ti-B-C-N, TiN and BCN coatings on silicon wafer at low substrate temperature of 350 °C. The coatings were deposited by magnetron sputtering of TiN and B_4C targets in the argon-nitrogen atmosphere at different nitrogen flow rates (F_{N2}). The structure, chemical bonding and mechanical properties were investigated. It was established that the Ti-B-C-N coatings represented the TiNC nanocrystallites (3.4 – 6.5 nm) embedded into the amorphous matrix that consists of the mixture of amorphous boron nitrogen (a-BN) and amorphous carbon (a-C). The coatings contain a small admixture of titanium oxides that are aggregated at the grain boundaries. The coatings deposited at high nitrogen flow rates were textured. An introduction of nitrogen prompts the formation of the TiNC crystallites of the TiN-TiC solid solutions and the a-BN amorphous tissue, which in turn causes the improvement of the mechanical properties of the Ti-B-C-N coatings. The best samples exhibited nanohardnes above 39 GPa. The nanocomposite Ti-B-C-N coatings deposited at comparatively low substrate temperatures (below 350 °C) could be recommended for an introduction to industry as wear-resistant and protective coatings.

ACKNOWLEDGEMENTS

This work was supported by the STCU Contract, No. 5539. We thank Dr. S.N. Dub for the nanoindentation of the samples and Dr. T. Tomila for the FTIR measurements.

REFERENCES

1. P.H. Mayrhofer, C. Mitterer, L. Hultman, H Clemens *Prog. Mater.* **51**, 1032 (2006).
2. P. Karvankova, M.G.J. Veprek-Heijman, D. Azinovic, S. Veprek, *Surf. Coat. Technol.* **200**, 2978 (2006).
3. P. Karvankova, M.G.J. Veprek-Heijman, O. Zindulka, A. Bergmaier, S. Veprek, *Surf. Coat. Technol.* **163-164**, 149 (2003).
4. J. Lin, B. Mishra, J.J. Moore, M. Pinkas, W.D. Sproul, *Surf. Coat. Technol.* **203**, 588 (2008).
5. X. Chen, Z. Wang, S. Ma, V. Ji, *Diamond and Related Materials* **19**, 1336 (2010).
6. G. Tang, X. Ma, M. Sun, S. Xu, *Surf. Coat. Technol.* **203**, 1288 (2009).
7. K.H. Kim, J.T. Ok, S. Abraham, Y.-R. Cho, In-W. Park, J.J. Moore, *Surf. Coat. Technol.* **201**, 4185 (2006).
8. P.C. Tsai, *Surf. Coat. Technol.* **201**, 5108 (2007).
9. H. Moreno, J.C. Caicedo, C. Amaya, J. Muñoz-Saldaña, L. Yate, J. Esteve, P. Prieto, *Appl. Surf. Sci.* **257**, 1098, (2010).
10. S.H. Lee, K.H. Nam, J.-W. Lim, J.-J. Lee, *Surf. Coat. Technol.* **174-175**, 758 (2003).
11. E. Galvanetto, F.P. Galliano, P. Borgioli, U. Bardi, A. Lavacchi, *Thin Solid Films* **384**, 223 (2001).
12. S. Zecout, S. Achour, A. Mosser, N. Tabet, *Thin Solid Films* **441**, 135 (2003).